Atmospheric Research 230 (2019) 104630

Contents lists available at ScienceDirect

Atmospheric Research

journal homepage: www.elsevier.com/locate/atmosres

Analysis of the atmospheric circulation pattern effects over SPEI drought index in Spain

Antonio Manzano[a], Miguel A. Clemente[b], Ana Morata[a], M. Yolanda Luna[a], Santiago Beguería[c], Sergio M. Vicente-Serrano[d], M. Luisa Martín[e,f,*]

[a] Agencia Estatal de Meteorología, Leonardo Prieto Castro, 8, 28040 Madrid, Spain
[b] Dpto. Astrofísica y Física de la Atmósfera, Facultad de Física, Universidad Complutense de Madrid, Ciudad Universitaria s/n, 28040 Madrid, Spain
[c] Estación Experiental de Aula Dei, Consejo Superior de Investigaciones Científicas, Avda. Montañana, 1005, 50059 Zaragoza, Spain
[d] Instituto Pirenaico de Ecología, Consejo Superior de Investigaciones Científicas, Avda. Montañana, 1005, 50059 Zaragoza, Spain
[e] Dpto. Matemática Aplicada, Escuela de Ingeniería Informática, Universidad de Valladolid, Pza. de la Universidad, 1, 40005 Segovia, Spain
[f] Instituto de Matemática Interdisciplinar, Universidad Complutense de Madrid, Ciudad Universitaria s/n, 28040, Spain

ARTICLE INFO

Keywords:
Droughts
Seasonal prediction
SPEI
Teleconnection patterns

ABSTRACT

Drought episodes affect large continental areas all over the world, becoming one of the main natural hazards regarding their economic, social and environmental impacts. The design and improvement of drought monitoring and forecasting systems has become a priority application and has driven the need to a better understanding of the development of drought episodes. In this work, a study of the relationships between drought conditions over the Iberian Peninsula and teleconnection patterns with a major impact over this region is assessed. The three-month aggregated standardized precipitation evapotranspiration index (SPEI) is used to characterize different clustered areas with homogeneous hydrological behaviour on a seasonal basis. Correlation results reveal that Artic Oscillation (AO) and North Atlantic Oscillation (NAO) patterns have a significant impact on droughts in winter over large areas of the Iberian Peninsula, while the Western Mediterranean Oscillation (WeMO) pattern exhibit the largest influence on hydrological behaviour over the southeastern region. The East Atlantic (EA) pattern effects switch between weakening and reinforcement as result of a balance of two different processes such as the increase in precipitation (dominant in winter) and the increase in temperature (dominant in summer). A wavelet analysis is performed to the seasonal mean atmospheric pattern time series and clustered mean SPEI time series. The wavelet power spectra highlight common periodicity features pointing out the close relationships between the atmospheric patterns and the drought index.

1. Introduction

A drought can be defined as a period of abnormally dry weather long enough to cause a serious hydrological imbalance (IPCC, 2014) due to a shortage of precipitation and/or an increase of evapotranspiration related to climatic factors as higher temperatures, lower relative humidity or strong winds (Wilhite, 2000). Persistent drought conditions reduce streamflow, reservoir and lake levels, snowpack, and groundwater levels and result in significant impacts on hydroelectric power production, recreation and tourism, irrigated agriculture, ecosystems, and other sectors (Wilhite and Pulwarty, 2018). Demand of water is expected to increase as population growth and its living standards improve (Bell, 2015).

Droughts affect more people than any other hazard (Hagman, 1984; Below et al., 2007) and, concerning the Iberian Peninsula, they are one of the main natural hazards regarding their economic and environmental impacts, with negative effects over crop yields, water resources, extension of forests or vegetation activity (Vicente-Serrano et al., 2017). These effects could be related with the occurrence and magnitude of forest fires over Spain, as found in other regions (Pompa-García et al., 2018). The current uncertainties regarding the recurrence of drought episodes and its economic, environmental and social impacts along with the recent past, present and future trends on a Climate Change context (Dai, 2011; Trenberth et al., 2014), justify the importance of the study of the drought in Spain.

The necessity of quantify the physical characteristics of drought has led to the definition of various indices, as the Standardized Precipitation Index (Mckee et al., 1993) or the Palmer Drought Severity

* Corresponding author at: Dpto. Matemática Aplicada, Escuela de Ingeniería Informática, Universidad de Valladolid, Pza. de la Universidad, 1, 40005 Segovia, Spain.
E-mail address: mlmartin@eii.uva.es (M.L. Martín).

https://doi.org/10.1016/j.atmosres.2019.104630
Received 10 May 2019; Received in revised form 19 July 2019; Accepted 22 July 2019
Available online 24 July 2019

Fig. 1. Physical map of the Iberian Peninsula.

Index (Palmer, 1965). These indices combine the information from meteorological and hydrological parameters such as precipitation, temperature or soil moisture in an attempt to characterize the occurrence and magnitude of drought episodes (Sheffield and Wood, 2011). The Standardized Precipitation Evapotranspiration Index (SPEI) is one of the most recently proposed indices (Vicente-Serrano et al., 2010; Beguería et al., 2014). The SPEI is calculated as the precipitation minus potential evapotranspiration for different temporal aggregation periods. By selecting the aggregation period the SPEI can be used for operational monitoring of different types of drought episodes. The SPEI takes both positive (precipitation surplus) and negative (drought scenario) values, a useful property to determine the onset and duration of drought episodes, and as a standardized index, it can be used for comparisons between regions. The inclusion of temperature information in the calculation of the SPEI via the potential evapotranspiration makes the SPEI a suitable index to assess the effects of climate change on droughts.

An increasing effort of both research and operational areas is being devoted to study and design seasonal drought forecasting methods for more effective prevention and adaptation strategies for drought impact mitigation (Turco et al., 2017). A better understanding of the relationships between the different atmospheric patterns and its impacts on droughts could help the enhancement and development of statistical and dynamic drought seasonal forecasting methodologies (Schubert et al., 2016; Ma et al., 2018; Hao et al., 2018).

The SPEI has been used in different areas of the world. Yao et al. (2019) used the SPEI and other drought indexes to identify drought events in China. They found that SPEI spatial and temporal patterns are mainly affected by topography and atmospheric circulation. Asong et al. (2018) analyzed drought behavior in Canada and established well-defined regions according with the drought time evolution and related them with the Pacific–North American (PNA) and Multivariate El Niño/Southern Oscillation Index (MEI). The SPEI has been also recently used in other studies such as evaluation of historical drought severity and their relationships with some atmospheric patterns (Byakatonda et al., 2018; de Oliveira-Júnior et al., 2018), analysis of intensity, spatial extent and frequency droughts (Mathbout et al., 2018), analysis of climate variation impacts on seasonal droughts reconstructing droughts using the SPEI (Shiru et al., 2019) and water resource availability (Hui-Mean et al., 2018). Concerning the SPEI studies in Europe, Kingston et al. (2015) used such drought index in order to analyze possible connections with some atmospheric circulation patterns in different European areas. As a result, they related the SPEI with combinations of the NAO and EA/WR circulation patterns on a monthly time scale. Spinoni et al. (2015) analyzed the biggest European drought events during 1950–2012 by means of various drought indices, highlighting differences in the drought frequency and intensity between northern and eastern Europe, and southern Europe and the Mediterranean area. Spinoni et al. (2017) investigated evolution of drought trends using SPEI and other indices over Europe, showing seasonally increase in the frequency and severity of droughts in different European regions.

In the current work, the relationships between the SPEI and relevant synoptic situations affecting the Iberian Peninsula hydrological variability are covered. These recurrent scenarios are characterized by teleconnection patterns (TPs). Thus, an analysis of the relationship between temporal evolution of the SPEI over the Iberian Peninsula and the TPs indices time series is assessed. Although a greater number of patterns has been considered, only those that have the greatest influence in the Iberian Peninsula (Rodríguez-Fonseca and Rodríguez-Puebla, 2010) are shown in this paper. These indices stand for the Artic Oscillation (AO), North Atlantic Oscillation (NAO), East Atlantic (EA), and West Mediterranean Oscillation (WeMO) patterns. Spatial distribution and temporal variability of the relationship between these large scale temperature and precipitation anomaly drivers and the SPEI drought index are studied. As a result, a new regionalization of the Iberian Peninsula based on meteorological drought is provided and common features between TP indices and mean within cluster SPEI values are identified by means of a correlation and wavelet analysis.

The study is organized as follows: a brief description of the SPEI dataset and TPs indices used is given in Section 2. The methodology is introduced in Section 3. Section 4 is devoted to show clustering, correlation and wavelet analysis results and give a causal explanation. A summary and discussion of the main results on the context of previous works is drawn in Section 5.

2. Datasets description

The SPEI database used in this works spans from 1962 to 2014 on a weekly basis and covers the Spanish territories within Iberian Peninsula

at 5.5 × 5.5 km spatial resolution (Vicente-Serrano et al., 2017). A map of the most relevant physical features of the domain under study is displayed in Fig. 1. The SPEI is derived from the precipitation and the potential evapotranspiration data sets based on temporal aggregation periods, that is, it is derived on each month taking into account the precipitation and potential evapotranspiration data from three previous months.

The temporal aggregation period for the computation of the SPEI database was carefully chosen. Different tests were conducted for aggregation times of 1, 3, 6 and 12 months. Results shows a higher correlation between the three-months aggregated SPEI (SPEI03 hereinafter) and the selected TPs, pointing out a predictive value of the SPEI on a seasonal basis. This three-month aggregation timescale corresponds to the usually referred as meteorological drought, caused mainly as a result of precipitation absolute amounts deficiencies over a certain period (Mckee et al., 1993).

The teleconnection patterns monthly indices series used in this work were obtained from NOAA website (NOAA, 2018) and Universitat de Barcelona (Universitat de Barcelona, 2018). A brief explanation of the selected TPs and their possible effects on droughts over the Iberian Peninsula is briefly given as follows:

- The *Artic Oscillation* (AO), also referred as the Northern Annular Mode (NAM), is defined as the projection of the first mode of empirical orthogonal functions (EOF) analysis using monthly mean 1000mb height anomaly data over 20°N-90°N to the daily anomaly 1000mb height field, also over 20°N-90°N. The AO represents the leading mode of variability of the extratropical Northern Hemisphere (Thompson and Wallace, 1998). When AO index is positive, the module of the geopotential anomalies increase and the circulation becomes more zonal, resulting on cyclones moving over high latitudes. This would lead to a predominance of high pressures over the Iberian Peninsula with associated scarce of precipitation and hence negative SPEI03 values. The opposite situation is expected with an AO negative phase, which promote paths for low pressure systems at lower latitude and associated western and southwestern winds carrying moist and precipitations to large parts of the territory. Thus, negative correlations between the AO and SPEI03 over wide areas of the Iberian Peninsula are expected to be found.
- The *North Atlantic Oscillation* (NAO) is a pressure dipole anomaly North-South which centers are located over Greenland and North Atlantic, between 35°N y 40°N (Barnston and Livezey, 1987). The NAO Index is calculated as the projection of the first mode of a rotated empirical orthogonal function analysis using monthly mean 500 mb height anomaly data over 0°N-90°N to the daily anomaly 500 mb height field, also over 0°N-90°N. Its behavior is similar to that of the AO and during the positive phase of the NAO a reduction in precipitation is expected over the Iberian Peninsula.
- The *East Atlantic* (EA) pattern was first identified by Wallace and Gutzler (1981) and it represents the second prominent mode of low-frequency variability over the North Atlantic. In this case, the anomaly centers are situated southeastward with respect to that of the NAO. The EA is linked with the subtropical dynamic through its southern center. During an EA positive phase, the western and southwestern winds reaching the Iberian Peninsula are reinforced, hence increasing precipitation over the Atlantic slope (Rodríguez-Fonseca and Rodríguez-Puebla, 2010). Furthermore, the EA pattern makes an impact over temperature, especially over the maxima, making not clear the role of the EA pattern over drought episodes (Sáenz et al., 2001; Frías et al., 2005).
- The *Western Mediterranean Oscillation* (WeMO) is obtained as the atmospheric pressure difference between Padua (45°23′N-11°52′E, north Italia) and San Fernando (36°28′N-6°12′W, southwest Spain). During positive phase, atmospheric pressure is anomalously high at San Fernando and low in Padua, promoting north-westerly fluxes over Iberian Peninsula which cause precipitation over Cantabrian areas and absence of precipitation over the Mediterranean regions. During negative phase, the pattern is reversed and the precipitation over the Mediterranean is enhanced (Martín-Vide and López-Bustins, 2006).

The main centers of these teleconnection patterns are present throughout the entire year. However, the teleconnection patterns are stronger during winter as they show a clearer signal and higher geopotential/index correlation. During summer, the teleconnection patterns weaken and in some cases their main centers are displaced, as occurs with NAO, for which the geopotential pattern moves towards the North.

It is important to note that in winter the precipitation (which dominates the SPEI03) over the Iberian Peninsula is mainly driven by advective circulation and consequently it is strongly related to the teleconnection patterns. This is not the case during summer, when the major part of the precipitation comes from convective processes and it is, therefore, less related to the teleconnection patterns. This seasonal difference on the main mechanism originating the precipitations, along with the summer weakened of the teleconnection patterns, is expected to lead to lower correlations in this season.

3. Methods

3.1. k-Means clustering

Hydrological behaviour over the Iberian Peninsula is not uniform, existing different hydroclimatic regions where precipitation regimes and their temporal variability vary as a function of the predominant circulation patterns (Zorita et al., 1992; Rodriguez-Puebla et al., 1998; Valero et al., 2009). These regions are also influenced by other factors such as their orography, orientation, coastal proximity or latitude (González-Hidalgo et al., 2011; Serrano-Notivoli et al., 2018).

In order to analyze the drought occurrence over the different regions and its relationship with the TPs, a *k*-means clustering technique was applied to the SPEI03 data (Lloyd, 1982; Arthur and Vassilvitskii, 2007). The k-means algorithm follow a series of steps: i) an a priori assumption on the number of clusters *k*; ii) random initialization (seeding) of each centroid between all the data series; iii) modification of the centroids in an iterative process until the mean Euclidean distances from the within-cluster data series respect to their corresponding centroid are minimized. The algorithm includes an iterative random seeding process in order to avoid local minima. As a result, areas of homogeneous SPEI03 values are obtained.

The a priori assumption on the number of clusters entails the imposition of a criterion to choose a particular number. Here, the elbow heuristic method is used: the location of a shift in the plot of the mean within-cluster sum of squares with respect to the numbers of clusters is set as the appropriate number of clusters (Bholowalia and Kumar, 2014).

3.2. Correlation analysis

A first approximation consisting in a comparison between the mean SPEI03 from each cluster and the TPs series is performed. Then, the monthly spatial correlation of the correlation between the whole SPEI03 dataset and the TPs is obtained. Significant correlation is determined via 95% confidence level t-Student based hypothesis test (Wilks, 2011). Values under 0.2 are filtered out. In order to explore the sturdiness of the results, the spatial distribution obtained is compared with the clusters SPEI03 mean values.

Additionally, in order to analyze the seasonal relationships between the drought index and the TPs, a cross-correlation analysis between SPEI03 index and TPs on a seasonal basis (DJF, MAM, JJA, SON) is also performed. Here, only results from SPEI03 monthly sampling versus the

TP seasonal mean are presented, as they show immediate interpretation and maximum correlation. The correlation value for a certain month corresponds to the obtained correlation between the SPEI03 value of such month and the seasonally mean TP index corresponding to the previous season.

3.3. Wavelet analysis

In order to analyze the temporal variability of droughts and its possible relationship with the TPs dominant frequencies, a wavelet transform analysis is carried out. Here, we apply a continuous wavelet transform with the most commonly used mother wavelet, the Morlet wavelet, which consists of a plane wave modulated by a gaussian envelope (Morlet et al., 1982; Büssow, 2007). Unlike other frequency analysis, e.g. Fourier transform, in which only frequency localization is given the continuous Morlet wavelet transform provide both frequency and time localization. This allows the identification of which are the dominant frequency in each month or year of the whole time series (Martín et al., 2011). By comparing the wavelet analysis for SPEI03 and TPs data within each cluster, the possible relation between them is studied taking into account a three months lag time.

The wavelet power spectrum diagrams shown in this study represent the squared module of the complex number given as a result of the wavelet transform of the signal. This representation can be understood as energy density and allows comparison with the spectral power of a Fourier transform (Büssow, 2007; Taylor et al., 2013).

4. Results

The k-means clustering technique is carried out for k number of clusters ranging from 3 to 15. As the number of clusters increases, the mean within-cluster sums of point-to-centroid distances diminishes following a potential behavior. This trend allows the elbow method to find that six is the appropriate number of clusters: a lesser number of clusters leads to a poorer spatial coherence whilst a higher number of clusters does not improve significantly the within-cluster cohesion.

As a result, six different well-defined regions of homogenous drought behavior characterized by the SPEI03 index are identified in the Iberian Peninsula for the three month timescale: southeast (SE), northeast (NE), northwest (NW), southwest (SW), center (CE) and Cantabrian (CA) (Fig. 2). Previous analysis suggested similar results using climatological precipitation data for SPI computation (Vicente-Serrano, 2006).

In order to explore the relationship between the TPs and the SPEI03 index, correlations between mean SPEI03 of each cluster and the TP time series are calculated. As a result, each TP shows correlation values

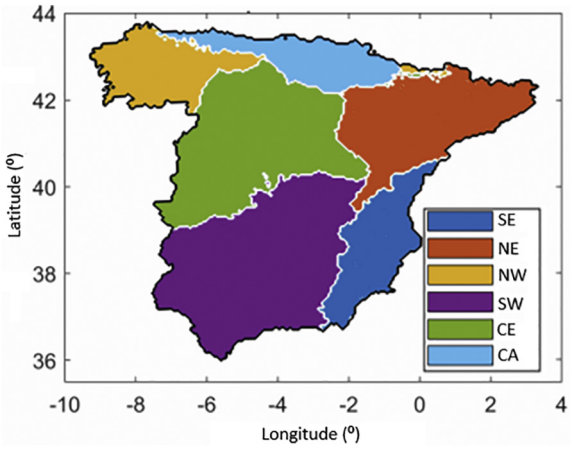

Fig. 2. Cluster distribution obtained by the *k*-means method applied to SPEI03 data.

with certain clusters, while magnitude or even the sign of the relationship vary throughout the year for most TPs (Fig. 3). Thus, AO, NAO and WeMO correlations (Fig. 3a, b, d) are weak in summer and EA correlations values change the sign (Fig. 3c). The highest correlations correspond to AO and NAO patterns from January to May for almost every cluster and the WeMO pattern (Fig. 3d) for SE and CA clusters on the same period. In this case, from November to May negative correlations with Mediterranean coastal clusters are observed, while the NW and CA clusters show positive correlations.

In order to further inspect the relationships between the teleconnection patterns and the SPEI03 index, monthly spatial correlation distributions are displayed. As an example, Fig. 4 shows the results for spatial correlations between March SPEI03 and the winter TPs, corresponding to the maximum observed in Fig. 3 for AO and NAO TPs. Results for AO and NAO patterns are very similar (Fig. 4a, b), with high negative correlations in extensive areas of the Iberian Peninsula. Nevertheless, the NAO pattern (Fig. 4b) does not affect the north (except the Pyrenees) and exhibit a major relationship along the Mediterranean Coast than the AO pattern, which shows no significant correlation in this region. The EA pattern (Fig. 4c) shows mainly positive correlations over the northwestern quadrant of the Iberian Peninsula. Finally, the WeMO pattern (Fig. 4d) shows bipolar distribution with negative values over the Mediterranean coastline and positive values along the Cantabrian basin. These results are consistent with the cluster analysis performed (Fig. 3).

The extent of significant correlation areas shown in Fig. 4 is computed as the percentage of grid points for which the positive/negative correlations are found significant. Results are shown in Fig. 5 accompanied by the mean value of the positive/negative correlations. The combined information from the mean correlations and the extent of the significant correlation areas allows the inference about how relevant a certain TP is over the SPEI03. As an example, the AO and NAO patterns exhibit high values of areal mean correlation and areal extent of the significant correlation from January to May: this indicates that the signal from both TPs is strong during these months over large areas of the territory. Nevertheless, this signal is weakened in summer, which is reflected in lower areal mean correlation values but also in the extent of the area of significant correlation. In the case of the EA pattern a switch of the sign is observed: areas with positive correlation between January and March disappear in April and wide areas of low but significant correlations develop instead.

Fig. 6 summarizes the area of significant correlations (computed as the sum of grid points with both positive and negative significant correlations) for all the TPs considered in this study throughout the year on a monthly basis. As mentioned above, the value for a particular month corresponds to the correlation between the SPEI03 value of the month considered and the mean TP index of the three months previous to that month. Here, the maximum significant correlation area of the AO, NAO, and WeMO patterns between January and May and its weakening during summer becomes more evident. The EA pattern exhibit more extensive correlation values in summer. Lower correlations are generally found in June, October and November. In the cases of October and November this might be due to the fact that in the three previous months (from July to October) large part of the rainfall is originated by convective processes. The opposite is observed from January to May, when the precipitation associated to the previous months is originated by advective situations which are directly related with the teleconnection patterns.

The analysis of the temporal variability of drought and its relationship with the TPs dominant frequencies is assessed by means of the wavelet decomposition of the mean within-cluster SPEI03 and that for the seasonal mean TPs. The most representative wavelets are shown in Fig. 7 and correspond to the highest correlation values from Fig. 3. Here, the wavelet power spectra displayed as a function of period and time correspond to winter TP and SPEI03 time series for March. The magnitude of wavelet coefficients gives a measure of the correlation

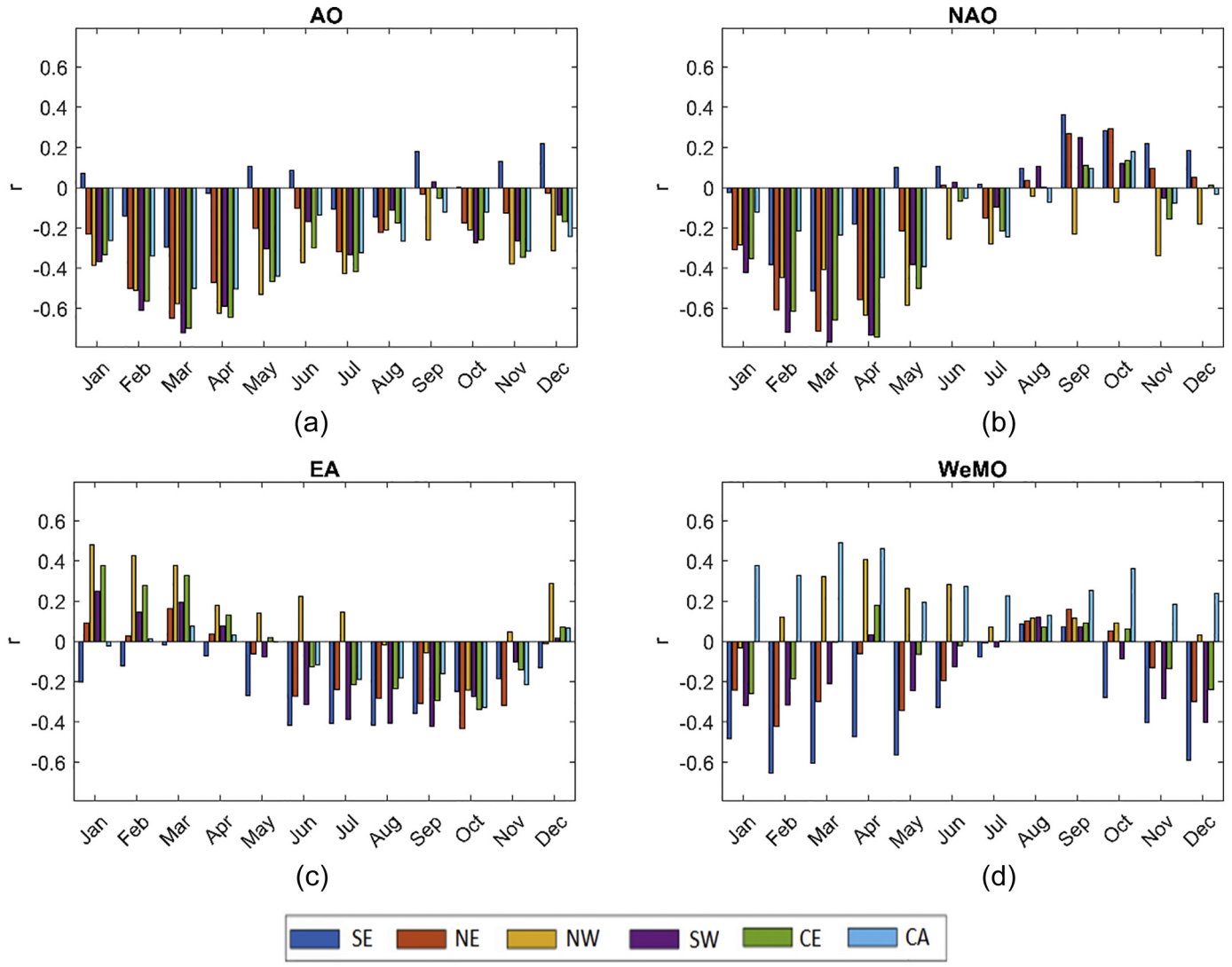

Fig. 3. Correlation between clusters mean SPEI03 and (a) AO; (b) NAO; (c) EA and (d) WeMO time series.

between the signal and the wavelet basis. The power spectrum in the AO (Fig. 7a) is mainly characterized by signal associated to 8 years throughout (1962–2014), displaying other highly energetic amplitudes around 5 and 3 years from 2000. Also a maximum nucleus between 1998 and 2010 is noticeable at periods lower than 3 years. It is remarkable how pronounced signals are similar to those shown in the wavelet power spectrum of SPEI03 of cluster CE (Fig. 7b), corresponding to the northern Iberian plain. The NAO power spectrum (Fig. 7c) shows similar signals with almost all clusters, with the exception of the SE cluster. The common signals becomes more evident with the SW cluster (Fig. 7d) at periods of 8 years from 1970 to 1990 and around 5 years from 1985 and 3 years from 2000. The power spectrum in the EA (Fig. 7e) shows signals at periods of 4 and 6 years throughout the whole time and around 3 years from mid 90s. These signals can be found in the NW cluster power spectrum (Fig. 7f). Finally, the WeMO power spectrum (Fig. 7g) reveals common signal with SE cluster (Fig. 7h) at periods between 3 and 6 years, especially noticeable from 2000.

Although similar results have been obtained in the remaining seasons (not shown), the common features between SPEI and TPs wavelets are more clearly identified during winter. As an example, the spring WeMO power spectrum exhibits a 7 year period signal throughout the whole time which is also found in the wavelet diagrams of June SE, NW and CA clusters. Furthermore, most signals weaken in summer which may be related with the convective origin of precipitation during this season.

5. Discussion and conclusions

The relationship between different TPs and the SPEI03 over Spain is studied. The spatial distribution of the correlations between them is analyzed and compared with the structure of the drought index clusters built as regions of well-defined homogeneous hydrological behavior. It is found that each cluster shows different response to the TPs throughout the year.

The AO pattern produces negative correlations in almost entire Iberian Peninsula, especially along Atlantic slope. A positive AO results in a blocking situation over the Iberian Peninsula, leading to a shortage of precipitation and negative SPEI03 values. In contrast, in the negative phase of the AO, the fronts passage and storms tracks take place further south affecting the Iberian Peninsula with westerly and southwesterly winds. These winds produce precipitations that are more intense in the Atlantic slope, while in the southeastern regions of the Peninsula the fronts arrive weakened and hardly precipitations take place due to a large scale Foehn's effect (Lana and Burgueño, 2000). Indeed, even positive correlations have been found in some months, which may be due to the long western continental wind path, which arrives the Mediterranean coasts dry and overheated, increasing potential

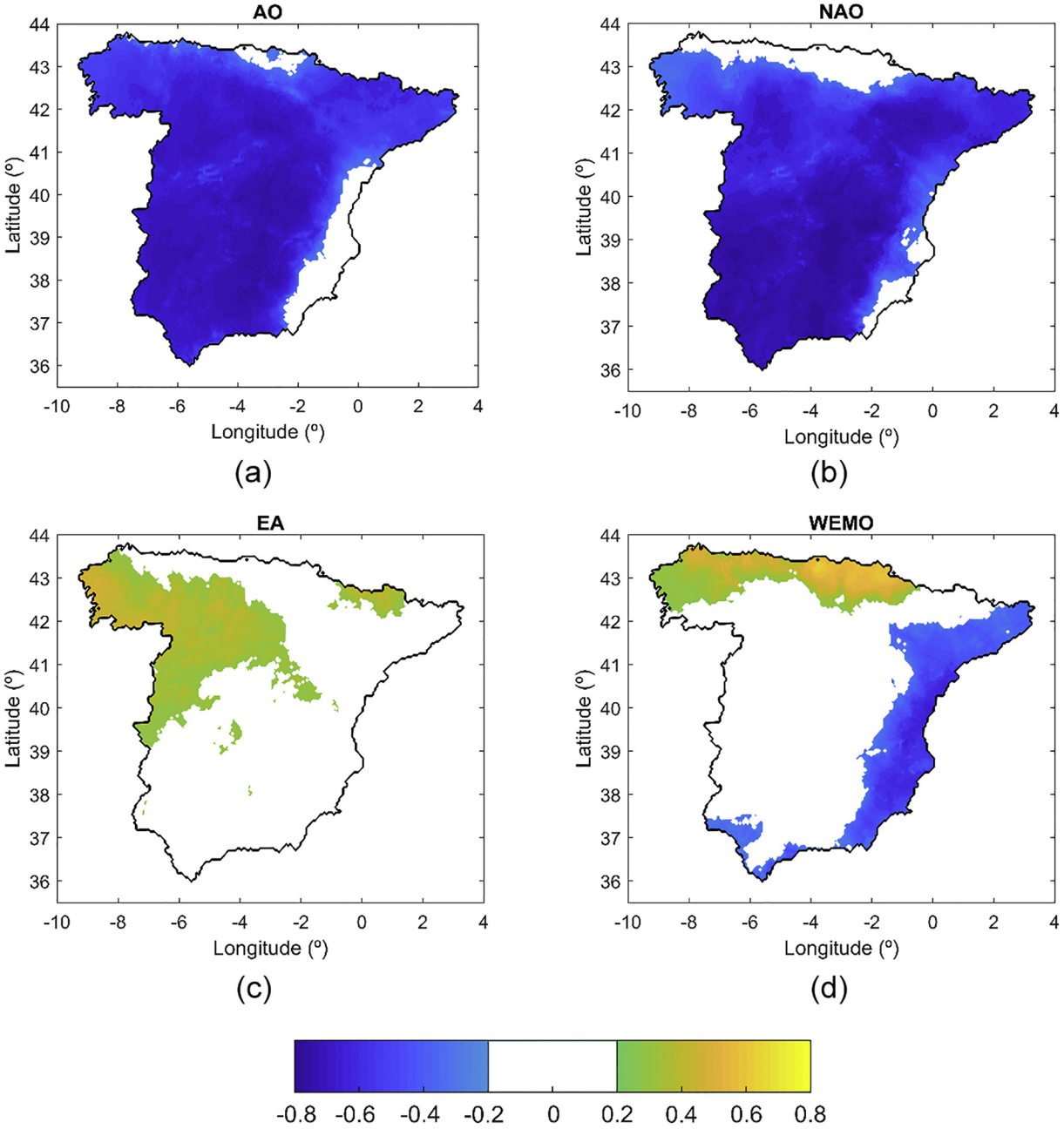

Fig. 4. Distribution of significant correlation between March SPEI03 and the winter (a) AO; (b) NAO; (c) EA and (d) WeMO patterns.

evapotranspiration. Another orographic effect is exhibited in the northern mountain systems, where the correlation values decay abruptly. This might be caused by the Foehn effect of the predominant southwesterly wind during negative AO phases that leads to decrease in precipitation and humidity and increase in temperature. The results showed that the relationship between the AO patterns and the SPEI03 is more intense and extensive in the months from January to April, when information of the AO between October and March is considered (remember that the monthly SPEI03 is computed aggregating data from previous 3 months). This responds to the fact that during winter the AO has a more intense signal and the origin of the precipitation in Iberian Peninsula is mainly advective due to the lack of energy to produce convection. In summer the opposite happens: the AO pattern and precipitation are mainly driven by connective processes which leads to a poor relationship between the TP and the SPEI03.

The effects of the NAO pattern on the SPEI03 in the Peninsula are similar for those of the AO pattern, as expected by its close relationship (Wallace, 2000), but slight differences arise: the magnitude of the correlations are lower in northern and northwestern areas and higher over south and northeastern regions. In addition, positive correlations during summer extend to more clusters. These differences may be due to the location of the anticyclonic action center during the negative phase of the NAO, which would produce storm tracks at a slightly lower latitude compared to the AO. These storms could even be associated with southeasterly winds before their passage (especially in the east and north of Iberian Peninsula) leading to an increase of precipitation in the Mediterranean slope and a shortage in the Cantabrian and northwest areas. Over the Northeast, the NAO pattern shows high negative correlations in the Ebro valley and less significant correlation in the Pyrenees area. The positive correlations exhibit in summer in the eastern area of the Iberian Peninsula may be due to the NAO pattern weakens in this season, bringing westerly winds characterized for being warmer and drier. In addition, in summer the centers of the NAO pattern move towards the north so that slightly lower pressures extend from the north

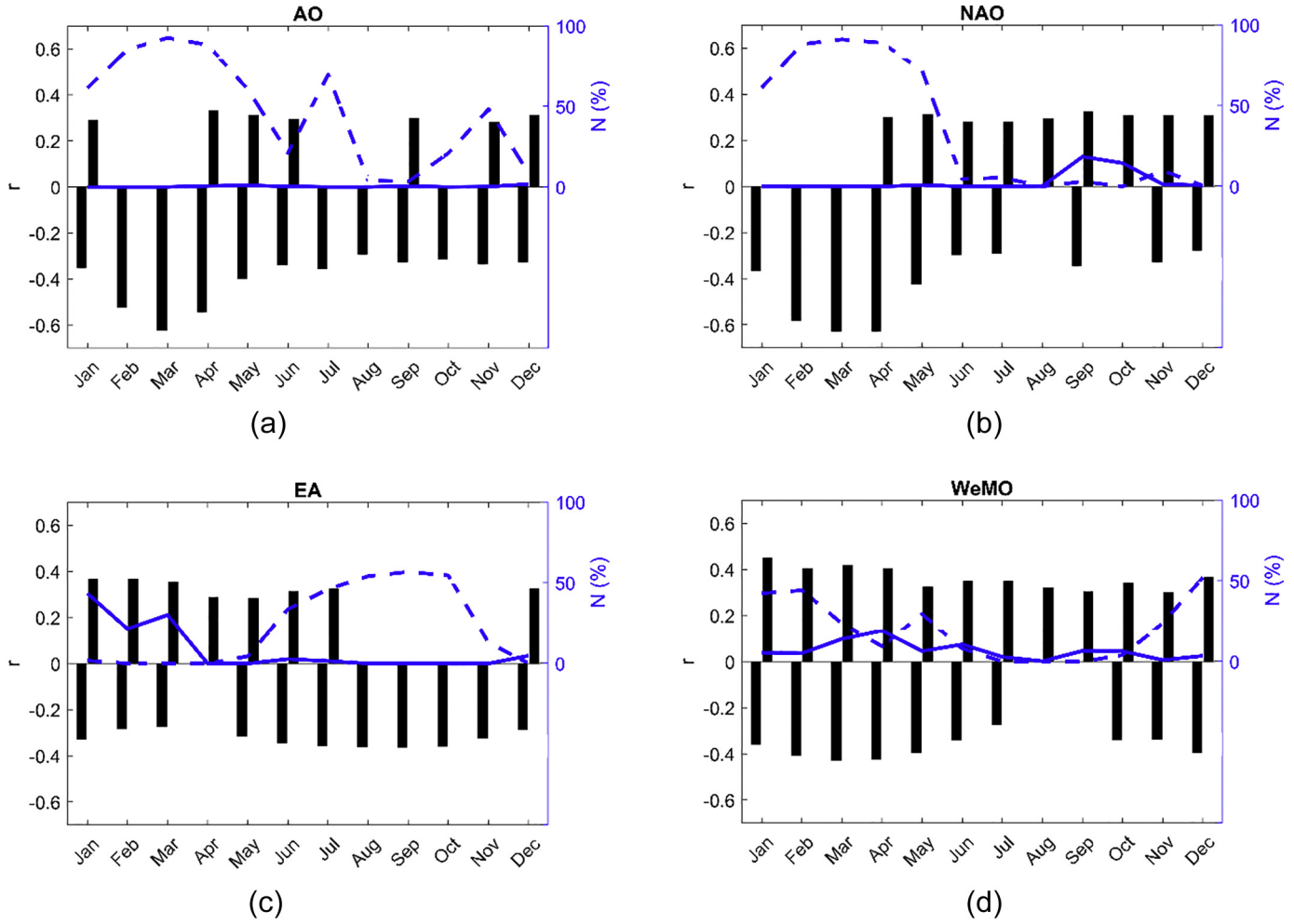

Fig. 5. Spatial mean value of significant correlations (bars) and areas of significant positive (continuous lines) and negative (dashed lines) correlations between SPEI03 and: (a) AO; (b) NAO; (c) EA and (d) WeMO patterns.

of Africa. By means of EOF analysis over the mean sea level pressure, Trigo and Palutikof (2001) found that the NAO pattern stands as the first mode, explaining a high percentage of the variance in the spatial domain covered in this work. It is therefore reasonable for this TP to account for much of the precipitation (and, hence, drought) over the Iberian Peninsula. Negative NAO-precipitation correlations from October to March were found by Martín-Vide and Fernández (2001), especially over the center and southwestern regions of the Iberian Peninsula. Similar results were obtained by Fernández-González et al. (2012), who related the decrease of winter precipitation (especially in March) with a positive trend in the NAO index during these months. In the current analysis, significant negative NAO-SPEI03 correlations span

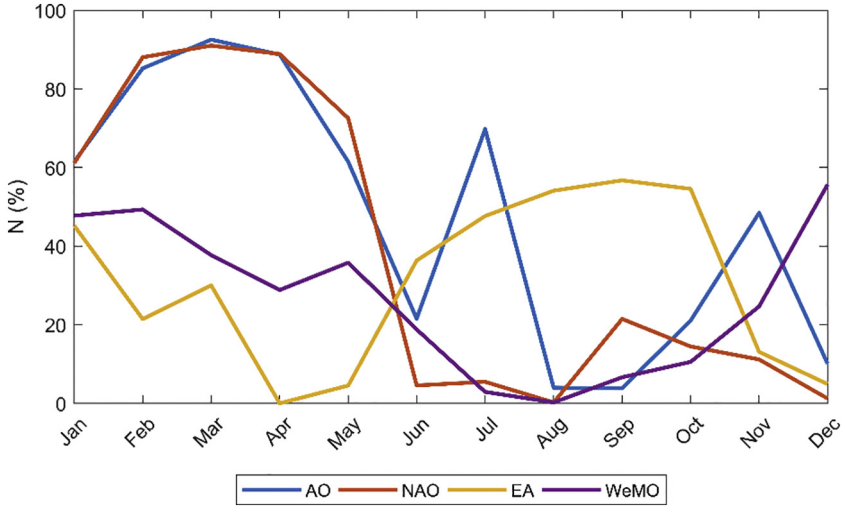

Fig. 6. Range of total significant correlation area (both positive and negative) between SPEI03 and TPs for each month as percentage with respect to total area.

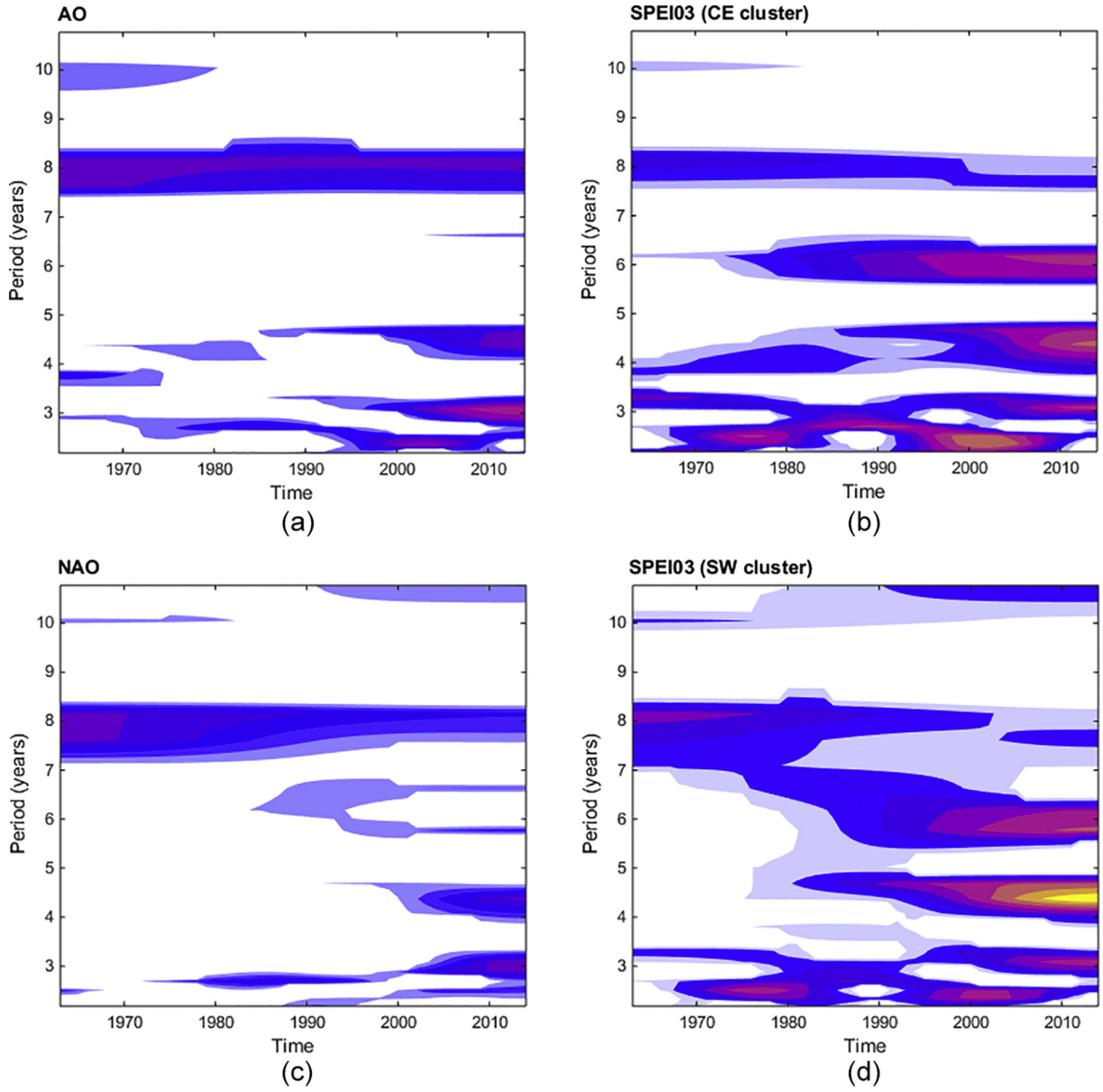

Fig. 7. Wavelet power spectra for winter TPs and March cluster mean SPEI03 of the cluster with higher correlation with each TP.

from January to May in almost the whole Iberian Peninsula with exception of the northern area.

The EA pattern shows positive correlations in winter and negative correlations in summer with gradual transition between both behaviors. The positive winter correlation values occur in the western half of the Iberian Peninsula, while the negative correlations spread over the most part of the territory during summer. The explanation of this features could rely on the prevailing southwesterly winds associated with the positive phase of the EA pattern which bring precipitations to the Atlantic slope. Southwesterly winds also bring high temperatures, although in winter they might not be high enough to produce relevant increase in evapotranspiration. In summer, the pattern weakens and the southwesterly winds do not bring as much moisture. This effect of the increase in evapotranspiration caused by high temperatures becomes predominant.

The WeMO pattern relationship with the SPEI03 over the Iberian Peninsula exhibits bipolar behavior, with negative correlations along the Mediterranean Sea coast and positive correlations over the Cantabrian Sea coast. These correlations are greater in the winter and spring months (from December to May). During the WeMO negative phase advection of easterly winds over the peninsula establishes. These winds bring humidity and precipitation to the Mediterranean slope. However, over the Bay of Biscay and the western areas of the peninsula these winds reach drier and warmer, leading to decrease in precipitation and an increase in evapotranspiration and promoting drought conditions. During the WeMO positive phase the prevailing winds have west and northwest component, giving rise to precipitation in the Cantabrian and northwestern areas and dry weather over the Mediterranean region. This bipolar pattern is especially clear from February to June, when precipitation in the Mediterranean area is maximum. Correlation values decrease considerably in summer due the scarce precipitation in the Mediterranean area and its origin mainly driven by convection. These results are in the same direction of those obtained by Martín-Vide and López-Bustins (2006), who pointed out that both the Northern and the Mediterranean façade show the greatest variability in precipitation based on the WeMO. By analyzing the wavelet power spectra diagrams of the winter WeMO and the SPEI03 in March in the SE cluster, shared signal with periodicities around 4 and 6 years can be found. The wavelet power spectrum of the SE cluster exhibits large discrepancies with the others TPs considered in this work,

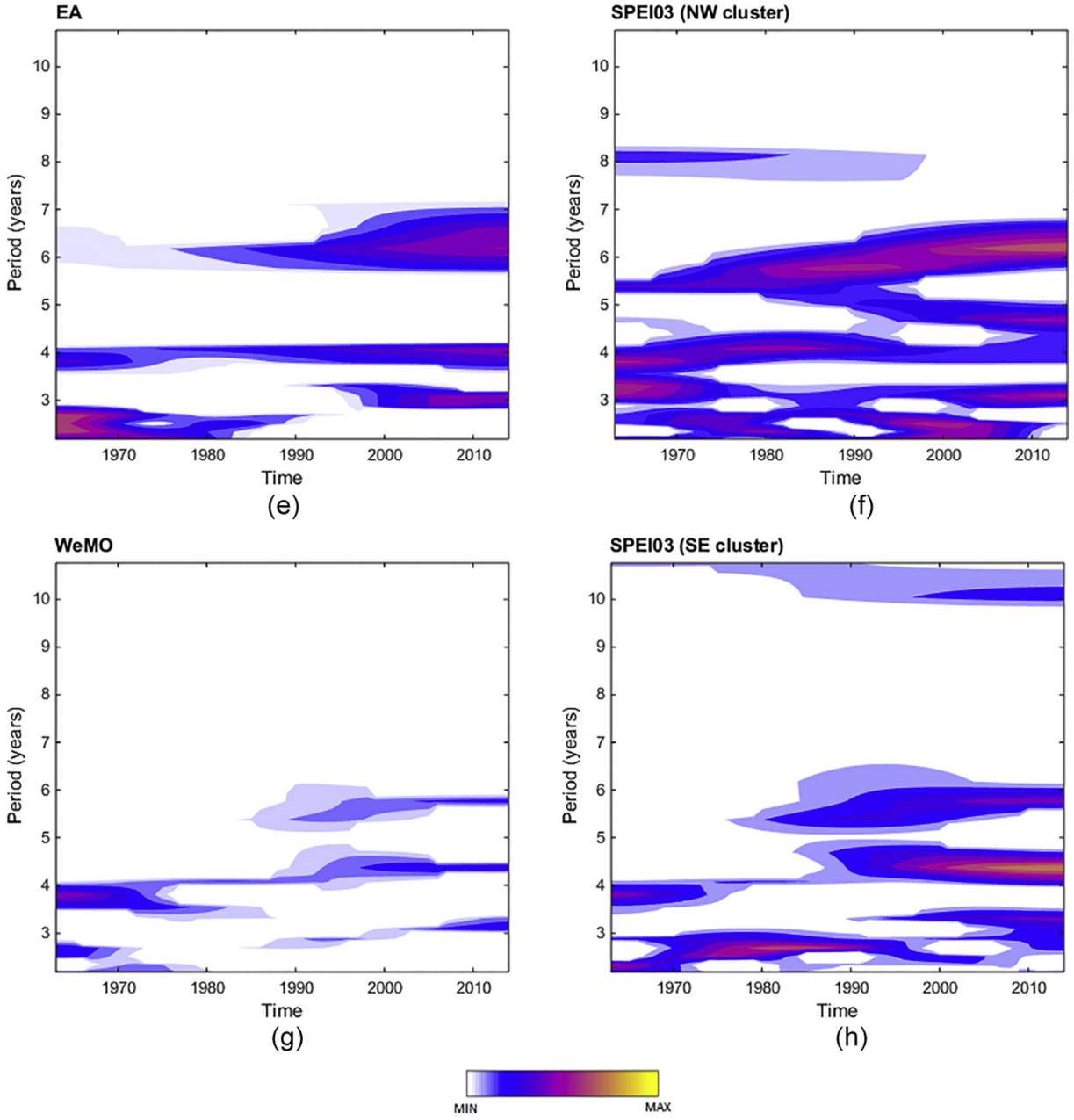

Fig. 7. (*continued*)

which points out the important role of the WeMO in the development of drought conditions in the southeastern peninsular region. Merino et al. (2015) used continuous wavelet transforms for examining periodicities of precipitation anomalies and their relation with the NAO pattern. They also found high coherence between precipitation anomalies and NAO on the Atlantic coast while the Mediterranean zone did not shown a strong relationship with such TP.

Summarizing, in this paper the spatio-temporal distribution of the SPEI03 over the Iberian Peninsula was analyzed, obtaining the following conclusions:

- Six different well-defined regions of homogenous drought behavior characterized by the SPEI03 index are identified. This result provide a new meteorological drought based regionalization of the Iberian Peninsula.
- Among the teleconnection patterns analyzed, those that showed the most significant correlation values with the SPEI03 index are, as expected, the AO and NAO patterns. These TPs explain the hydrological behavior in the winter months in large part of the territory, since the correlations are very extensive and high.
- The WeMO stands as the pattern that most clearly explains the hydrological behavior in the eastern peninsula area, which is also one of the regions where droughts are more recurrent and their impacts are more severe.
- In addition, The EA pattern relationship with SPEI03 was analyzed in this work. This TP was found to present positive correlations in winter and negative correlations in summer, as result of a balance of two different processes such as the increase in precipitation (dominant in winter) and the increase in temperature (dominant in summer).
- The wavelet analysis of the teleconnection pattern time series is compared to those applied to the cluster mean SPEI03 index time series. Wavelet power spectra showed common periodicity features which point out the close relationship between both signals, especially in winter. Wavelet analysis should be applied to SPEI series at different temporal aggregation periods in order to further inspect

these relationships.

The results obtained in this work may be useful for decision-making in human activities such as agriculture, hydrology and tourism. This paper could be useful in monitoring of drought episodes based on the knowledge of specific synoptic atmospheric patterns as suitable for development of drought episodes on particular areas of the Iberian Peninsula.

Acknowledgements

This work was been partially supported by research projects DESEMON (CGL2014-52135-C3-2-B), PCIN-2014-013-C07-04, PCIN2016-080 (UE ERA-NET Plus NEWA Project), CGL2016-78702-C2-1-R and CGL2016-78702-C2-2-R, CGL2016-81828-REDT and the ECMWF special projects (SPESMART and SPESVALE). The authors wish to thank the NOAA and Universitat de Barcelona for providing the datasets.

References

Arthur, D., Vassilvitskii, S., 2007. k-Means++: the advantages of careful seeding. In: Proceedings of the Eighteenth Annual ACM-SIAM Symposium on Discrete Algorithms, pp. 1027–1035.

Asong, Z.E., Wheater, H.S., Razavi, S., Bonsal, B., Kurkute, S., 2018. Historical drought patterns over Canada and their teleconnections with large-scale climate signals. Hydrol. Earth Syst. Sci. 22 (6), 3105–3124.

Barnston, A.G., Livezey, R.E., 1987. Classification, seasonality and persistence of low frequency atmospheric circulation patterns. Mon. Weather Rev. 115, 1083–1126.

Beguería, S., Vicente-Serrano, S.M., Reig, F., Latorre, B., 2014. Standardized precipitation evapotranspiration index (SPEI) revisited: parameter fitting, evapotranspiration models, tools, datasets and drought monitoring. Int. J. Climatol. 34 (10), 3001–3023.

Bell, S., 2015. Renegotiating urban water. Elsevier J. Progr. Plann. 96, 1–28.

Below, R., Grover-Kopec, E., Dilley, M., 2007. Documenting drought-related disasters: a global reassessment. J. Environ. Dev. 16 (3), 328–344.

Bholowalia, P., Kumar, A., 2014. EBK-Means: a clustering technique based on elbow method and K-means in WSN. Int. J. Comput. Appl. 105 (9), 17–24.

Büssow, R., 2007. An algorithm for the continuous Morlet wavelet transform. Mech. Syst. Signal Process. 21 (8), 2970–2979.

Byakatonda, J., Parida, B.P., Moalafhi, D.B., Kenabatho Piet, K., 2018. Analysis of long term drought severity characteristics and trends across semiarid Botswana using two drought indices. Atmos. Res. 213, 492–508. https://doi.org/10.1016/j.atmosres.2018.07.002.

Dai, A., 2011. Drought under global warming: a review. Wiley Interdiscip. Rev. Clim. Chang. 2, 45–65.

de Oliveira-Júnior, J.F., de Gois, G., de Bodas Terassi, P.M., da Silva Junior, C.A., Blanco, C.J.C., Sobral, B.S., Gasparini, K.A.C., 2018. Drought severity based on the SPI index and its relation to the ENSO and PDO climatic variability modes in the regions North and Northwest of the State of Rio de Janeiro - Brazil. Atmos. Res. 212, 91–105. https://doi.org/10.1016/j.atmosres.2018.04.022.

Fernández-González, S., Del Río, S., Castro, A., Penas, A., Fernández-Raga, M., Calvo, A., Fraile, R., 2012. Connection between NAO, weather types and precipitation in León, Spain (1948-2008). Int. J. Climatol. 32 (14), 2181–2196. https://doi.org/10.1002/joc.2431.

Frías, M.D., Fernández, J., Sáenz, J., Rodríguez-Puebla, C., 2005. Operational predictability of monthly average maximum temperature over the Iberian Peninsula using DEMETER simulations and downscaling. Tellus Ser. A 57 (3), 448–463.

González-Hidalgo, J.C., Brunetti, M., de Luis, M., 2011. A new tool for monthly precipitation analysis in Spain: MOPREDAS database (monthly precipitation trends December 1945–November 2005). Int. J. Climatol. 31, 715–731.

Hagman, G., 1984. Prevention Better than Cure: Report on Human and Natural Disasters in the Third World. Swedish Red Cross, Stockholm.

Hao, Z., Singh, V.P., Xia, Y., 2018. Seasonal drought prediction: advances, challenges, and future prospects. Rev. Geophys. 56, 108–141.

Hui-Mean, F., Yusop, Z., Yusof, F., 2018. Drought analysis and water resource availability using standardized precipitation evapotranspiration index. Atmos. Res. 201, 102–115. https://doi.org/10.1016/j.atmosres.2017.10.014.

IPCC, 2014. In: Core Writing Team, Pachauri, R.K., Meyer, L.A. (Eds.), Annex II: Glossary. [Mach, K. J., S. Planton and C. von Stechow (eds.)] Climate Change 2014: Synthesis Report. Contribution of Working Groups I, II and III to the Fifth Assessment Report of the Intergovernmental Panel on Climate Change. IPCC, Geneva, Switzerland, pp. 117–130.

Kingston, D.G., Stagge, J.H., Tallaksen, L.M., Hannah, D.M., 2015. European-scale drought: understanding connections between atmospheric circulation and meteorological drought indices. J. Clim. 28, 505–516.

Lana, X., Burgueño, 2000. Some statistical characteristics of monthly and annual pluviometric irregularity for the spanish mediterranean coast. Theor. Appl. Climatol. 65, 79–97.

Lloyd, S., 1982. Least squares quantization in PCM. IEEE Trans. Inf. Theory 28, 129–137.

Ma, F., Luo, L., Ye, A., Duan, Q., 2018. Seasonal drought predictability and forecast skill in the semi-arid endorheic Heihe River basin in northwestern China. Hydrol. Earth Syst. Sci. 22, 5697–5709.

Martín, M.L., Valero, F., Morata, A., Luna, M.Y., Pascual, A., Santos-Muñoz, D., 2011. Springtime coupled modes of regional wind in the Iberian Peninsula and large-scale variability patterns. Int. J. Climatol. 31 (6), 880–895.

Martín-Vide, J., Fernández, D., 2001. El índice NAO y la precipitación mensual en la España peninsular. Investig. Geogr. (26), 41–58.

Martín-Vide, J., López-Bustins, J.A., 2006. The Western Mediterranean Oscillation and rainfall in the Iberian Peninsula. Int. J. Climatol. 26, 1455–1475.

Mathbout, S., Lopez-Bustins, J.A., Martin-Vide, J., Bech, J., Rodrigo, F.S., 2018. Spatial and temporal analysis of drought variability at several time scales in Syria during 1961–2012. Atmos. Res. 200, 153–168. https://doi.org/10.1016/j.atmosres.2017.09.016.

Mckee, T.B., Doesken, N.J., Kleist, J., 1993. The relationship of drought frequency and duration to time scales. In: AMS 8th Conference on Applied Climatology, pp. 179–184 January.

Merino, A., López, L., Hermida, L., Sánchez, J.L., García-Ortega, E., Gascón, E., Fernández-González, S., 2015. Identification of drought phases in a 110-year record from Western Mediterranean basin: Trends, anomalies and periodicity analysis for Iberian Peninsula. Glob. Planet. Chang. 133, 96–108. https://doi.org/10.1016/j.gloplacha.2015.08.007.

Morlet, J., Arens, G., Fourgeau, E., Glard, D., 1982. Wave propagation and sampling theory | part I: complex signal and scattering in multilayered media. Geophysics 47 (2), 203–221.

NOAA, 2018. Climate Indices: Monthly Atmospheric and Ocean Time Series. Retrieved June 2, 2018 from. https://www.esrl.noaa.gov/psd/data/climateindices/list/.

Palmer, W.C., 1965. Meteorological drought. In: U.S. Weather Bureau Res. Paper No. 45.

Pompa-García, M., Camarero, J.J., Rodríguez-Trejo, D.A., Vega-Nieva, D.J., 2018. Drought and spatiotemporal variability of forest fires across Mexico. Chin. Geogr. Sci. 28 (1), 25–37.

Rodríguez-Fonseca, B., Rodríguez-Puebla, C., 2010. Climate teleconnections affecting Iberian peninsula climate variability. Predictability and expected changes. Climate in Spain: past, present and future. Region. Clim. Change Assess. Rep. 1, 53–68.

Rodriguez-Puebla, C., Encinas, A.H., Nieto, S., Garmendia, J., 1998. Spatial and temporal patterns of annual precipitation variability over the Iberian Peninsula. Int. J. Climatol. 18, 299–316.

Sáenz, J., Rodríguez-Puebla, C., Fernández, J., Zubillaga, J., 2001. Interpretation of interannual winter temperature variations over southwestern Europe. J. Geophys. Res. Atmos. 106 (D18), 20641–20651.

Schubert, S.D., Stewart, R.E., Wang, H., Barlow, M., Berbery, E.H., Cai, W., Hoerling, M.P., Kanikicharla, K.K., Koster, R.D., Lyon, B., Mariotti, A., Mechoso, C.R., Müller, O.V., Rodriguez-Fonseca, B., Seager, R., Seneviratne, S.I., Zhang, L., Zhou, T., 2016. Global meteorological drought: a synthesis of current understanding with a focus on SST drivers of precipitation deficits. J. Clim. 29 (11), 3989–4019.

Serrano-Notivoli, R., Martín-Vide, J., Saz, M.A., Longares, L.A., Beguería, S., Sarricolea, P., Meseguer-Ruiz, O., de Luis, M., 2018. Spatio-temporal variability of daily precipitation concentration in Spain based on a high-resolution gridded data set. Int. J. Climatol. 38, 518–530.

Sheffield, J., Wood, E.F., 2011. Drought: Past Problems and Future Scenarios. Earthscan, London, Washington, DC.

Shiru, M.S., Shahid, S., Chung, S.-S., Alias, N., 2019. Changing characteristics of meteorological droughts in Nigeria during 1901–2010. Atmos. Res. 223, 60–73. https://doi.org/10.1016/j.atmosres.2019.03.010.

Spinoni, J., Naumann, G., Vogt, J.V., Barbosa, P., 2015. The biggest drought events in Europe from 1950 to 2012. J. Hydrol. Reg. Stud. 3, 509–524. https://doi.org/10.1016/j.ejrh.2015.01.001.

Spinoni, J., Naumann, G., Vogt, J.V., 2017. Pan-European seasonal trends and recent changes of drought frequency and severity. Glob. Environ. Chang. 148, 112–130.

Taylor, G.W., McCarley, R.W., Salisbury, D.F., 2013. Early auditory gamma band response abnormalities in first hospitalized schizophrenia. Suppl. Clin. Neurophysiol. 62, 131–145.

Thompson, D.W.J., Wallace, J.M., 1998. The Arctic Oscillation signature in the wintertime geopotential height and temperature fields. Geophys. Res. Lett. 25, 1297–1300.

Trenberth, K.E., Dai, A., van der Schrier, G., Jones, P.D., Barichivich, J., Briffa, K.R., Sheffield, J., 2014. Global warming and changes in drought: expectations, observations and uncertainties. Nat. Clim. Chang. 4, 17–22.

Trigo, R.M., Palutikof, J.P., 2001. Precipitation scenarios over Iberia: a comparison between direct GCM output and different downscaling techniques. J. Clim. 14 (23), 4422–4446.

Turco, M., Ceglar, A., Prodhomme, C., Soret, A., Toreti, A., Francisco, J.D.-R., 2017. Summer drought predictability over Europe: empirical versus dynamical forecasts. Environ. Res. Lett. 12 (8), 084006.

Universitat de Barcelona, 2018. La Oscilación de la Mediterránea Occidental (WeMO). Retrieved June 2, 2018 from. http://www.ub.edu/gc/es/2016/06/08/wemo/.

Valero, F., Martín, M.L., Sotillo, M.G., Morata, A., Luna, M.Y., 2009. Characterization of the autumn Iberian precipitation from long-term datasets: comparison between observed and hindcasted data. Int. J. Climatol. 29, 527–541.

Vicente-Serrano, S.M., 2006. Differences in spatial patterns of drought on different timescales: an analysis of the Iberian Peninsula. Water Resour. Manag. 20, 37–60.

Vicente-Serrano, S.M., Beguería, S., López-Moreno, J.I., 2010. A multiscalar drought index sensitive to global warming: the standardized precipitation evapotranspiration index. J. Clim. 23 (7), 1696–1718.

Vicente-Serrano, S.M., Tomás-Burguera, M., Beguería, S., Reig-Gracia, F., Latorre, B., Peña-Gallardo, M., Luna, Y., Morata, A., González-Hidalgo, J.C., 2017. A high resolution dataset of drought indices for Spain. Data 2 (3), 22.

Wallace, J.M., 2000. North Atlantic oscillation/annular mode: two paradigms-one phenomenon. Q. J. R. Meteorol. Soc. 126 (564), 791–805.
Wallace, J.M., Gutzler, D.S., 1981. Teleconnections in the Geopotential Height Field during the Northern Hemisphere Winter. Mon. Weather Rev. 109, 784–812.
Wilhite, D.A., 2000. Drought: A Global Assessment. vol. I. Routledge, pp. 3–18 Chap. 1.
Wilhite, D.A., Pulwarty, R.S. (Eds.), 2018. Drought and Water Crises: Integrating Science, Management, and Policy. CRC Press, Boca Raton (Chap. 1).
Wilks, D.S., 2011. Statistical Methods in the Atmospheric Sciences, Volume 100. Academic press, pp. 467.
Yao, J., Tuoliewubieke, D., Chen, J., Huo, W., Hu, W., 2019. Identification of drought events and correlations with large-scale ocean–atmospheric patterns of variability: a case study in Xinjiang, China. Atmosphere 10 (2), 94.
Zorita, E., Kharin, V., Von Storch, H., 1992. The atmospheric circulation and sea surface temperature in the North Atlantic area in winter: their interaction and relevance for Iberian precipitation. J. Clim. 5, 1097–1108.